Experimental Brain Research (2020) 238:807–824
https://doi.org/10.1007/s00221-020-05746-6

RESEARCH ARTICLE

Normoxic post-ROSC ventilation delays hippocampal CA1 neurodegeneration in a rat cardiac arrest model, but does not prevent it

Gerburg Keilhoff[1] · Maximilian Titze[1] · Henning Rathert[1] · Benjamin Lucas[2] · Torben Esser[3] · Uwe Ebmeyer[3]

Received: 1 October 2019 / Accepted: 3 February 2020 / Published online: 3 March 2020

Abstract
The European Resuscitation Guidelines recommend that survivors of cardiac arrest (CA) be resuscitated with 100% O_2 and undergo subsequent—post-return of spontaneous circulation (ROSC)—reduction of O_2 supply to prevent hyperoxia. Hyperoxia produces a "second neurotoxic hit," which, together with the initial ischemic insult, causes ischemia–reperfusion injury. However, heterogeneous results from animal studies suggest that normoxia can also be detrimental. One clear reason for these inconsistent results is the considerable heterogeneity of the models used. In this study, the histological outcome of the hippocampal CA1 region following resuscitation with 100% O_2 combined with different post-ROSC ventilation regimes (21%, 50%, and 100% O_2) was investigated in a rat CA/resuscitation model with survival times of 7 and 21 days. Immunohistochemical stainings of NeuN, MAP2, GFAP, and IBA1 revealed a neuroprotective potency of post-ROSC ventilation with 21% O_2, although it was only temporary. This limitation should be because of the post-ROSC intervention targeting only processes of ischemia-induced secondary injury. There were no ventilation-dependent effects on either microglial activation, reduction of which is accepted as being neuroprotective, or astroglial activation, which is accepted as being able to enhance neurons' resistance to ischemia/reperfusion injury. Furthermore, our findings verify the limited comparability of animal studies because of the individual heterogeneity of the animals, experimental regimes, and evaluation procedures used.

Keywords Astroglia · Cardiac arrest/resuscitation · Hippocampus · Hyperoxia · Microglia · Normoxia

Introduction

The existing guidelines recommend ventilating survivors of cardiac arrest (CA) during resuscitation with 100% O_2 [European Resuscitation Guidelines (Soar et al. 2015)]. Moreover, they suggest that, to prevent hyperoxia, the O_2 supply should be reduced following return of spontaneous circulation (ROSC) to obtain an arterial O_2 saturation of 94–98%. Hyperoxic reperfusion is known to produce a "second hit" that is even more neurotoxic than the initial ischemic insult; together, they cause ischemia–reperfusion injury [IR; (Francis and Baynosa 2017)]. A key event of IR is the generation of reactive oxygen species (ROS) such as superoxide and hydroxyl radicals. These can damage cells via either direct DNA damage or membrane lipid peroxidation. Thus, reduction of the O_2 supply, leading to decreased ROS production, should represent a promising therapeutic approach [21% (normoxic) O_2 supply: (Marsala et al. 1992; Zwemer et al. 1995; Liu et al. 1998; Vereczki et al. 2006; Brucken et al. 2010; Hazelton et al. 2010; Solberg et al. 2010, 2012; Solevag et al. 2010; Walson et al. 2011)]. The existing guidelines have been confirmed by Patel et al. (2018). They found that, in adults with CA, intra-arrest hyperoxia is associated with lower mortality, whereas post-arrest hyperoxia is associated with higher mortality. Other researchers (Young et al. 2014) preferred oxygen titration only after ROSC and arrival in hospital. However, there is evidence that normoxia can also be detrimental. Cerebral

Communicated by Thomas Deller.

✉ Gerburg Keilhoff
gerburg.keilhoff@med.ovgu.de

[1] Institute of Biochemistry and Cell Biology, Medical Faculty, University of Magdeburg, Leipziger Strasse 44, 39120 Magdeburg, Germany

[2] Department of Trauma Surgery, Medical Faculty, University of Magdeburg, Magdeburg, Germany

[3] Department of Anesthesiology, Medical Faculty, University of Magdeburg, Magdeburg, Germany

histopathology after reoxygenation with normoxic room air has been shown to be as bad as that after reoxygenation with 100% O_2 (Temesvari et al. 2001).

Considering these findings, we examined the histological outcome of the hippocampal CA1 region resulting from hyperoxic (100% O_2) resuscitation combined with post-ROSC ventilation using different concentrations of oxygen (21%, 50%, and 100%) in our well-established rat asphyxia cardiac arrest/reperfusion (ACA/R) model. The animals' survival times (STs) were 7 and 21 days. We used immunohistochemical stainings of NeuN, MAP2, GFAP, and IBA1 in varying combinations. Analysis of the respective mean values of staining in the different experimental groups revealed a potent neuroprotective effect of normoxic post-ROSC ventilation (21% O_2). However, this neuroprotection was only temporary. Over longer STs, this neuroprotective effect disappeared completely, and the neurodegenerative potency of normoxic post-ROSC ventilation became as high as that of hyperoxic post-ROSC ventilation.

In addition, we extended the focus on the individual heterogeneity of test rats following ACA/R. In a systemic review "Contemporary animal models of cardiac arrest" (Vognsen et al. 2017), it was explained that "the great heterogeneity of these models along with great variability in definitions and reporting make comparisons between studies difficult". Consistently, the authors called for standardization of animal CA research and reporting. Along with the many technical parameters, standardization of which is difficult but possible, individual heterogeneity of test animals is worth observing. However, it is usually ignored in favor of statistical group comparison. Our analysis of the individual pattern of vital parameters and staining profiles verified the need to consider the great individual heterogeneity of laboratory animals as a variable in ACA/R animal models and their interpretation.

Materials and methods

Animals

Ethical approval for this study was granted according to the requirements of the German Animal Welfare Act on the Use of Experimental Animals and the Animal Care and Use Committees of Saxony-Anhalt (permit number 42502-2-2-947 Uni MD). Animals from the institute's breeding population of inbred Wistar rats (Harlan-Winkelmann; Borchen, Germany) were housed under controlled laboratory conditions (12 h light/12 h dark cycle, lights on at 6:00 a.m.; temperature 20 °C ± 2 °C; air humidity 55–60%), with free access to water and chow. Great care was taken to minimize both the number of animals used in the experiments and the amount of suffering they endured.

A total of 59 age-matched (15 weeks, 300–350 g) male rats were divided into the following groups:

(i) Sham-operated (ST: 7 days, ventilation with 50% O_2).
(ii) ACA/R-treated (ST: 7 days; reoxygenation with 21% O_2).
(iii) ACA/R-treated (ST: 7 days, reoxygenation with 50% O_2).
(iv) ACA/R-treated (ST: 7 days, reoxygenation with 100% O_2).
(v) ACA/R-treated (ST: 21 days, reoxygenation with 21% O_2).
(vi) ACA/R-treated (ST: 21 days, reoxygenation with 50% O_2).
(vii) ACA/R-treated (ST: 21 days, reoxygenation with 100% O_2).

The effect of different O_2 concentrations on sham animals after both STs was assessed in a pilot experiment. No differences were found, so we examined only a 7-day-sham group with 50% O_2 as the standard ventilation regime for 1 h post-preparation.

We began with 5 animals in the sham group and 54 ACA/R-treated animals. Twenty-four of the ACA/R animals were excluded (see below). Finally, we analyzed 5 animals per group; 35 rats in total.

Intervention protocol

Anesthesia [sevoflurane; Pfizer GmbH, Berlin, Germany; 5% in an oxygen/nitrous oxide mixture (40:60)] was delivered via facemask until the completion of endotracheal intubation with a modified laryngoscope and the placement of a venous catheter for muscular relaxation with vecuronium (1 mg/kg; Pfizer). Animals were treated with intermittent positive pressure ventilation (IPPV). For drug administration, blood sampling, and continuous blood pressure monitoring, both left femoral vessels were cannulated with polyethylene catheters. After 5 min of room air ventilation (anesthetic washout) and baseline control, asphyxia was induced via end-expiratory interruption of IPPV on paralyzed rats for 6 min. Within ~ 3 min, the animals went into ACA (defined as a non-pulsatile blood pressure lower than 10 mmHg).

Resuscitation was commenced by administering epinephrine (i.v.; 1 µg/kg; Pfizer) and sodium bicarbonate (1 mEq/kg) under a 100% oxygen supply, accompanied by manual external chest compression (200/min). Once ROSC, defined as a pulsatile mean arterial pressure (MAP) higher than 60 mmHg, was achieved, the oxygen supply was varied to either 21%, 50%, or 100% for 1 h. Animals with no ROSC within 2 min were excluded (24 in total, and 8 of them without ROSC). The 2-min interval is our laboratory standard to avoid non-homogeneous ACA/R periods causing

pathophysiological differences and resulting in more animals being required. We monitored vital parameters (ECG, blood pressure, temperature, and airway pressure) continuously during the first 45 min of the post-resuscitation intensive-care phase. At 5, 15, 30, and 45 min after ROSC, we collected arterial blood samples and analyzed them for the blood gases pCO_2 and pO_2, pH, HCO_3^- concentration, and glucose. Subsequently, catheters were removed, cannulated vessels were ligated, incisions were closed surgically, and the animals were extubated and returned to their cages. To exclude neuroprotective effects of hypothermia, we used a heating mat to maintain body temperature at 37 °C ± 0.3 °C during preparation, insult, and the first 45 min post-ROSC. The animals' normal body temperature was then maintained by placing them in an incubator cage for 24 h.

Assessment of hippocampal CA1 histology

Following 7 and 21 days' ST, we sacrificed anaesthetized rats by transcardial perfusion with 0.4% 0.1 M phosphate-buffered paraformaldehyde (PFA, pH 7.4, Millipore, Darmstadt, Germany). The brains were removed quickly and post-fixed in the same fixative overnight at 4 °C. Following 2 days' cryoprotection in 30% sucrose (in 0.4% PFA; pH 7.4), the brains were frozen rapidly at − 20 °C, sliced on a cryostat (Jung Frigocut 2800 E, Leica, Bensheim, Germany; sagittal, 20 µm), and immuno-stained with different mixtures of primary antibodies (diluted in 10% fetal calf serum and 0.3% Triton-X 100 in PBS; all chemicals were from Sigma-Aldrich, Taufkirchen, Germany): (i) mouse monoclonal anti-NeuN (neuronal nuclei antibody, MAB377; Chemicon, Billerica, USA; 1:100), (ii) polyclonal rabbit anti-GFAP (glial fibrillary acidic protein, 10555; Progen, Heidelberg, Germany; 1:500), (iii) monoclonal mouse anti-MAP2 (microtubule-associated protein 2, SMI-52R; Covance, Münster, Germany; 1:1.000); and (iv) rabbit polyclonal anti-IBA1 (ionized calcium binding adaptor molecule 1, 019–19741; WAKO Chemicals, Neuss, Germany; 1:1.000). The secondary antibodies' mixture comprised goat anti-mouse Alexa 488 (green, A28175; Invitrogen, Carlsbad, USA; 1:500) and donkey anti-rabbit Cy3 (red, 711-165-152; Dianova, Hamburg, Germany; 1:500). We diluted the mixture in 1% normal goat serum and 0.3% Triton-X in PBS. Nuclei were counter-stained with DAPI (4′,6-diamidino-2-phenylindole, 62,248, Thermo Scientific, Waltham, MA, USA; 1:1.000, 5 min). Cryo-sections were mounted on slides, embedded with Immu-Mount (Thermo Scientific), and examined under an AxioImager.M1 fluorescent microscope (Zeiss, Jena, Germany) with Plan-Neofluar fluorescein/rhodamine objectives.

Therefore, 5 alternating slices/staining/animal were scanned image field by image field (objective 40/0.75×, 63/1.4) to create an image of the complete hippocampus (1388 × 900 pixel; AxioVision software "Panorama", Zeiss). Then, according to the ImageJ user manual (http://rsbweb.nih.gov/ij/), we calculated the integrated density (Widmer et al. 2007) of the respective staining in the CA1 region (including the Stratum oriens, the Stratum pyramidale, the Stratum radiatum, and the Stratum lacunosum moleculare). ID was given as CTCF [corrected total cell fluorescence = (ID − (selected area × mean fluorescence of background)) × 10^{-5}] in arbitrary units. Moreover, CA1 pyramidal cells were semi-quantified. Therefore, we measured the CA1 layer length using ImageJ software by drawing a line freehand through the center of the cell bodies in the layer. All clearly NeuN-positive cells were counted. Dividing the number of cells by the CA1 layer length provided the respective linear density (LD; pyramidal cells/mm) (Louis et al. 2013). Each time, we calculated a mean per animal and used it as one value for the statistical analyses.

Statistical analysis

The quantitative data [presented either as the mean ± SD (Fig. 1) or as a boxplot (Fig. 4)] were analyzed via the non-parametric Kruskal–Wallis test and the Dunn's multiple comparison post hoc test using Graph Pad Prism 6 (GraphPad Software Inc., La Jolla, CA, USA). A p value of ≤ 0.05 was considered as indicative of statistical significance.

We assessed the relationships between vital parameters (pO_2, pCO_2, HCO_3^-, pH, BE, MAP, HF, and glucose) and hippocampal CA1 histology (in the form of GFAP, IBA1, MAP2 and NeuN immunohistochemical staining intensity) as well as those between pO_2 and the other vital parameters (pCO_2, HCO_3^-, pH, BE, MAP, HF, and glucose) by means of linear regression analysis, and we compared significant differences in the slope with zero. In general, a p value of ≤ 0.05 was considered as indicative of statistically significant differences.

Results

Effect of ACA/R with different post-ROSC O_2 concentrations on vital parameters

Preparing the rats, including anesthesia via facemask, trachea intubation, cannulation of the left femoral vessels, and determination of the baseline vital parameters, took 24 ± 5 min. In the process, the vital parameters were affected only marginally; they were all within the physiological ranges (baseline, BL). ACA/R induced a significant, though transitory, increase of MAP returning rapidly to baseline values (Fig. 1a) and an insignificant increase of heart rate (Fig. 1b). The arterial CO_2 tension (pCO_2; Fig. 1c) and the blood glucose values (Fig. 1d) exhibited ventilation-dependent courses, but there were no significant differences to the

A MAP (mmHg)

	sham	21 % O_2	50 % O_2	100 % O_2
BL	89 ± 13	79 ± 18	78 ± 16	79 ± 18
5 min	95 ± 10	134 ± 25**	157 ± 23***	171 ± 16***
15 min	91 ± 11	74 ± 27§§	83 ± 27§§§	95 ± 22
30 min	93 ± 9	76 ± 23§§§	73 ± 18§§§	83 ± 20§§
45 min	97 ± 10	75 ± 22§§	70 ± 18§§§	82 ± 20§§

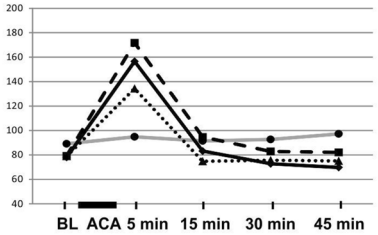

B heart rate (min^{-1})

	sham	21 % O_2	50 % O_2	100 % O_2
BL	368 ± 46	321 ± 30	309 ± 24	315 ± 20
5 min	357 ± 31	414 ± 44	407 ± 37	427 ± 32
15 min	361 ± 31	357 ± 37	348 ± 55	332 ± 35
30 min	370 ± 55	338 ± 43	324 ± 50§§	319 ± 33§§
45 min	375 ± 46	336 ± 46	302 ± 37§§	300 ± 28§§§

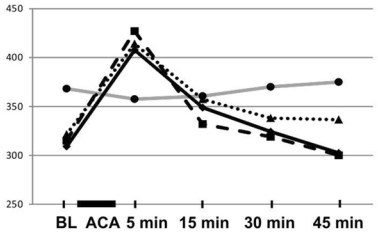

C pCO_2 (mmHg)

	sham	21 % O_2	50 % O_2	100 % O_2
BL	40 ± 3	36 ± 9	37 ± 9	43 ± 4
5 min	40 ± 5	57 ± 21	50 ± 18	46 ± 9
15 min	41 ± 3	49 ± 12	46 ± 12	46 ± 15
30 min	40 ± 2	45 ± 15	43 ± 5	47 ± 17
45 min	41 ± 1	41 ± 9	41 ± 5	43 ± 12

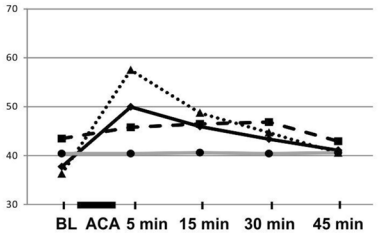

D glucose (mmol/l)

	sham	21 % O_2	50 % O_2	100 % O_2
BL	11 ± 5	10 ± 3	10 ± 3	12 ± 2
5 min	12 ± 5	15 ± 3	14 ± 4	15 ± 2
15 min	12 ± 5	16 ± 4	13 ± 5	14 ± 3
30 min	11 ± 4	13 ± 6	10 ± 3	11 ± 3
45 min	11 ± 4	9 ± 3	9 ± 3	10 ± 3§

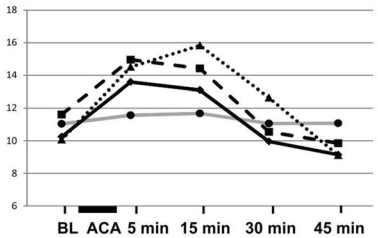

E pH

	sham	21 % O_2	50 % O_2	100 % O_2
BL	7.41 ± 0.05	7.41 ± 0.07	7.39 ± 0.05	7.39 ± 0.04
5 min	7.40 ± 0.02	7.21 ± 0.08 $^{\#/****}$	7.23 ± 0.15 ****	7.23 ± 0.08 *
15 min	7.39 ± 0.02	7.30 ± 0.08	7.28 ± 0.08*	7.29 ± 0.10
30 min	7.39 ± 0.02	7.35 ± 0.09	7.35 ± 0.07	7.34 ± 0.09
45 min	7.39 ± 0.02	7.38 ± 0.07§§	7.36 ± 0.05§	7.37 ± 0.08§

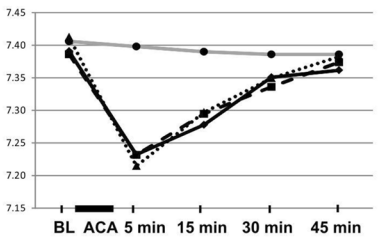

F pO_2 (mmHg)

	sham	21 % O_2	50 % O_2	100 % O_2
BL	172 ± 33	151 ± 32	156 ± 27	166 ± 32
5 min	172 ± 29	74 ± 57	119 ± 30	261 ± 93^{+}
15 min	175 ± 26	89 ± 51	139 ± 38	361 ± 104^{++}
30 min	177 ± 17	117 ± 60	144 ± 27	394 ± 159^{+}
45 min	178 ± 17	94 ± 50	156 ± 32	411 ± 140^{++++}

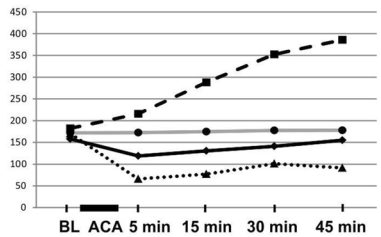

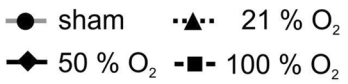

intra-group comparison
vs. BL: *p < 0.05; **p < 0.005; ***p < 0.001; ****p < 0.0001
vs. 5 min: §p < 0.05 §§p < 0.005; §§§p < 0.001;
between-group comparison
ACA/R (n = 10/ventilation regime) vs. sham (n = 5): $^{\#}$p < 0.05
ACA/R 100 % vs. ACA/R 21 %: $^{+}$p < 0.05; p^{++} < 0.01; $^{++++}$p < 0.0001

◂**Fig. 1** Pre- and post-resuscitation physiological parameters. The arterial pO_2 offered significant ventilation-dependent differences; 100% O_2 ventilation implied the highest pO_2 values consistently, whereas 21% and 50% O_2 ventilation produced pO_2 values below the sham group values. *BL* base line, *MAP* mean arterial pressure, pCO_2 arterial carbon dioxide tension, pO_2 arterial oxygen tension, *ACA* asphyxia cardiac arrest. Data: mean ± SD; in the graphs, the presentation of SD has been omitted for the benefit of better clarity; non-parametric Kruskal–Wallis/Dunn's multiple comparison post-hoc test

respective sham course. At 5 min post-ROSC, the pH levels of the 3 ACA/R groups were significantly lower (Fig. 1e). As anticipated, the arterial pO_2 of the ACA/R rats displayed ventilation-dependent courses (Fig. 1f); the values of the group with 100% O_2 ventilation were consistently greater than were the respective values of all the other groups, whereas the values of the 21% group and the 50% group were lower than those of the sham group. There was no effect on the body temperature (tympanal and rectal) within the 45-min monitoring periods post- resuscitation (data not shown). There was no correlation observed between the time of ROSC and the pattern of the pO_2 status (Table 1).

Figure 2 depicts linear regression analysis of pO_2 and the further vital parameters (MAP, HF, pCO_2, glucose, HCO_3^-, pH or BE) for the various O_2 ventilation regimes. Different results were obtained depending on the values used. If the mean values for each experimental group/parameter were used, there was negative correlation in the sham group between pO_2 and both HCO_3^- (Fig. 2d) and BE (Fig. 2g); the higher the pO_2, the lower both HCO_3^- and BE. We found no correlations in the 21% (Fig. 2h–n) and 100% O_2 (Fig. 2v–z″) ventilation groups. However, in the 50% O_2 ventilation group, there were significant correlations related to all parameters (Fig. 2o–u), and pO_2 was positively correlated with both HCO_3^- (Fig. 2d vs. r) and BE (Fig. 2g vs. u). Analysis of the regression lines, which describe the nature of the relationship between the parameters, reveals that the pattern of the parameters in the sham group is opposite to that of almost all the ACA/R groups. Only 3 exceptions display the same relationship as the respective sham parameter; these are pCO_2 of the 100% O_2 ventilation regime (Fig. 2x) and the glucose values of both the 50% (Fig. 2s) and the 100% (Fig. 2z) O_2 ventilation regimes.

The correlation patterns changed when we worked with the individual values for each animal within one experimental group. In the sham group, pO_2 correlated with heart rate and MAP (Fig. 3a, b). In the 21% O_2 ventilation group, pO_2 correlated with pCO_2 (Fig. 3j), glucose (Fig. 3l), and pH (Fig. 3m). The correlations of pO_2 with pH, HCO_3^-, BE, and glucose were lost in the 50% O_2 ventilation group, the remaining correlations being with MAP (Fig. 3o), heart rate (Fig. 3p), and pCO_2 (Fig. 3q). In the 100% O_2 ventilation group, pO_2 correlated with pCO_2 (Fig. 3x) and pH (Fig. 3z′). Only pCO_2 was correlated (negatively) with pO_2 in all ACA/R groups (Fig. 3j, q, x). Such correlation was absent from the sham group (Fig. 3c). Comparison of the correlation patterns of mean values with individual values reveals that some regression lines and, thus, the nature of the parameter relationships have been changed. In the sham group, the mean values of base excess correlated negatively (even significantly) with pO_2, whereas the respective individual values showed a rising regression line (Fig. 2g vs. Fig. 3g). Such reversion could be found also in the case of the sham group heart rate (Fig. 2b vs. Fig. 3b), HCO_3^- (Fig. 2d vs. Fig. 3d) and glucose (Fig. 2e vs. Fig. 3e), but it was much rarer in the ACA/R groups. Here, it could be seen in the case of glucose in the 21% O_2 ventilation group (Fig. 2l vs. Fig. 3l) and of pCO_2 in the 100% O_2 ventilation group (Fig. 2x vs. Fig. 3x). These results support the need to consider the individual heterogeneity of test animals, which is (too) often overlooked in the statistical group comparison.

Effect of ACA/R with different post-ROSC O_2 concentrations on hippocampal CA1 histology

Figure 4 presents an overview of the morphometric analysis of the different stainings. Figure 5 presents an overview of the immunohistological patterns. The co-stainings NeuN-IBA1 and MAP2-GFAP are shown. After 21 days' ST, the neuronal parameter NeuN (Fig. 4a) showed significant neurodegeneration when compared with the animals in the sham group. Ventilation with 21% O_2 appeared to delay neurodegeneration. However, with increasing ST, the neurodegenerative potency of 21% O_2 ventilation adapted to that of the 50% and 100% O_2 ventilation groups. The NeuN-IBA1 co-immunostaining reflected very well the process of CA1 pyramidal cell loss and the respective microglia activation (Fig. 5b1–g2). MAP2, a marker of the neuronal dendritic network (Fig. 4b), implied that dendrite degeneration happened earlier. Here, significances between the sham and the ACA/R groups were found after 7 days' ST, whereby ventilation with 21% O_2 failed to achieve significance. The simultaneous to dendritic degeneration activation of microglia (IBA1 staining; Fig. 4c) was evident in the Strata radiatum and lacunosum moleculare in all ACA/R groups (Fig. 5b1–g2), but it achieved significance only in the long-term survival groups (Fig. 5e1–g2). Analysis of GFAP-expressing astroglia revealed a significant reactive gliosis in all long-term survival groups (Figs. 4d, 5i1–n2).

The diagrams in Fig. 4 indicated that the laboratory animals showed individual heterogeneity. Thus, we analyzed the individual neurodegenerative status and set it in relation to the respective individual O_2 status (Table 1). First, we realized the heterogeneity of individual O_2 status within equal ventilation groups. Furthermore, the O_2 status did not enable explicit prediction of the neurodegenerative outcome. Thus, in the normoxic group with short ST the highest

Table 1 Neurodegenerative status of hippocampal CA 1 region in dependence on ROSC and O_2-status

	ROSC (s)	pO_2-status (mmHg)					Neurodegenerative status of hippocampal CA 1 region
		BL	5′	15′	30′	45′	
Sham; 7 days; 50% O_2							
Rat 1	–	161	166	172	167	160	
Rat 2	–	132	140	144	175	191	
Rat 3	–	223	218	215	205	198	
Rat 4	–	177	180	179	177	178	
Rat 5	–	167	158	163	163	162	
7 days; 21% O_2							
Rat 6	40	185	48	65	65	75	Massive cell and no dendrite loss
Rat 7	45	100	165	161	190	178	No cell and moderate dendrite loss
Rat 8	20	142	47	138	144	76	Moderate cell and massive dendrite loss
Rat 9	20	139	26	39	44	45	Moderate cell and massive dendrite loss
Rat 10	25	177	49	56	135	99	Moderate cell and dendrite loss
7 days; 50% O_2							
Rat 11	31	151	74	99	119	188	Massive cell and dendrite loss
Rat 12	24	76	76	90	171	179	Moderate cell and massive dendrite loss
Rat 13	20	198	112	127	110	144	Moderate cell and massive dendrite loss
Rat 14	25	165	110	96	138	178	Massive cell and dendrite loss
Rat 15	25	177	149	146	138	178	Minimal cell and massive dendrite loss
7 days; 100% O_2							
Rat 16	64	234	140	129	139	294	Massive cell and dendrite loss
Rat 17	25	235	91	65	131	334	Moderate cell and dendrite loss
Rat 18	33	156	145	146	308	332	Moderate cell and dendrite loss
Rat 19	35	225	194	324	466	522	Massive cell and dendrite loss
Rat 20	30	204	158	243	214	215	Moderate cell and dendrite loss
21 days; 21% O_2							
Rat 21	30	229	29	36	55	76	Massive cell and dendrite loss
Rat 22	31	214	32	38	44	49	Massive cell and moderate dendrite loss
Rat 23	30	153	171	160	167	148	Moderate cell and massive dendrite loss
Rat 24	20	165	52	58	95	100	Massive cell and dendrite loss
Rat 25	32	166	107	78	129	94	Massive cell and dendrite loss
21 days; 50% O_2							
Rat 26	27	107	81	77	118	192	Massive cell and dendrite loss
Rat 27	28	164	169	161	157	154	Moderate cell and massive dendrite loss
Rat 28	33	202	129	160	174	173	Moderate cell and massive dendrite loss
Rat 29	28	139	95	153	143	113	Massive cell and dendrite loss
Rat 30	20	153	87	142	137	130	Massive cell and dendrite loss
21 days; 100% O_2							
Rat 31	55	213	354	368	368	405	Moderate cell and dendrite loss
Rat 32	22	186	209	255	197	203	Massive cell and dendrite loss
Rat 33	30	143	152	256	307	378	Massive cell and dendrite loss
Rat 34	20	151	363	459	602	577	Moderate cell and massive dendrite loss
Rat 35	25	139	229	471	497	496	Massive cell and dendrite loss

s seconds

arterial pO_2 status led to low neuronal degeneration (rat 7). However, the patterns were lost entirely in the normoxic group with longer ST.

We found no correlation between time of ROSC and neurodegenerative outcome (Table 1). A slow recovery did not necessarily result in massive neurodegeneration (e.g., rat 7) and a fast recovery did not guarantee little neurodegeneration (e.g., rat 30). We found equivalent neurodegenerative

Fig. 2 Linear regression analysis of the relationship between the independent variable pO_2 and the dependent variables in the form of vital parameters (VP) using the mean values of each experimental group. *r* correlation coefficient indicating strength and direction of the linear relationship between pO_2 and the respective VP; positive slope: pO_2 and VP change in the same direction; negative slope: pO_2 and VP change in opposite directions; $*p<0.05$; $**<0.005$: significant linear dependencies between pO_2 and VP. Please note the different symbols of the data points indicating their affiliation to the time of measurement (BL, 5, 15, 30, and 45 min)

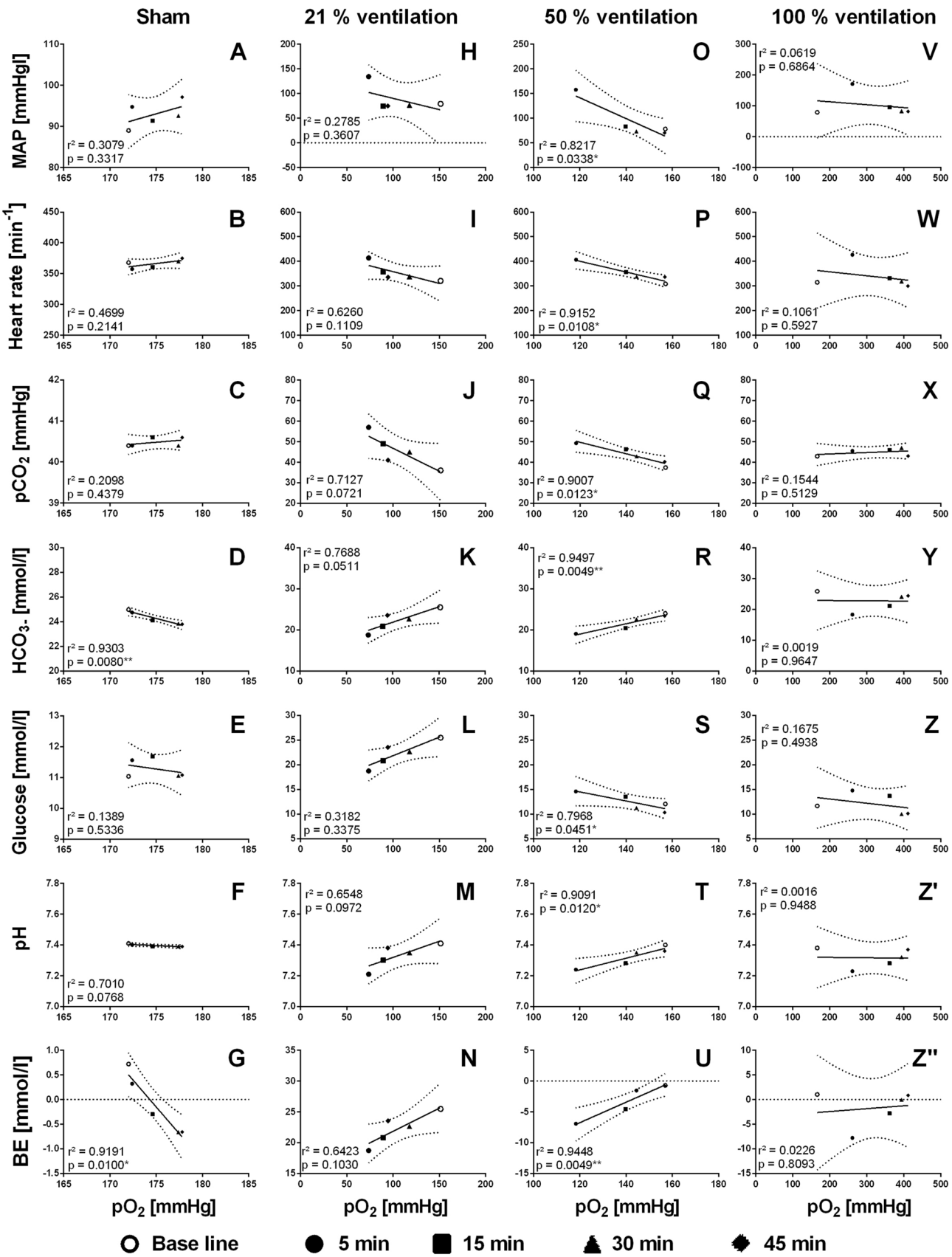
Sham
21 % ventilation
50 % ventilation
100 % ventilation
MAP [mmHgl]
Heart rate [min-1]
pCO2 [mmHg]
HCO3- [mmol/l]
Glucose [mmol/l]
pH
BE [mmol/l]
A r² = 0.3079 p = 0.3317
H r² = 0.2785 p = 0.3607
O r² = 0.8217 p = 0.0338*
V r² = 0.0619 p = 0.6864
B r² = 0.4699 p = 0.2141
I r² = 0.6260 p = 0.1109
P r² = 0.9152 p = 0.0108*
W r² = 0.1061 p = 0.5927
C r² = 0.2098 p = 0.4379
J r² = 0.7127 p = 0.0721
Q r² = 0.9007 p = 0.0123*
X r² = 0.1544 p = 0.5129
D r² = 0.9303 p = 0.0080**
K r² = 0.7688 p = 0.0511
R r² = 0.9497 p = 0.0049**
Y r² = 0.0019 p = 0.9647
E r² = 0.1389 p = 0.5336
L r² = 0.3182 p = 0.3375
S r² = 0.7968 p = 0.0451*
Z r² = 0.1675 p = 0.4938
F r² = 0.7010 p = 0.0768
M r² = 0.6548 p = 0.0972
T r² = 0.9091 p = 0.0120*
Z' r² = 0.0016 p = 0.9488
G r² = 0.9191 p = 0.0100*
N r² = 0.6423 p = 0.1030
U r² = 0.9448 p = 0.0049**
Z'' r² = 0.0226 p = 0.8093
pO2 [mmHg]
Base line
5 min
15 min
30 min
45 min

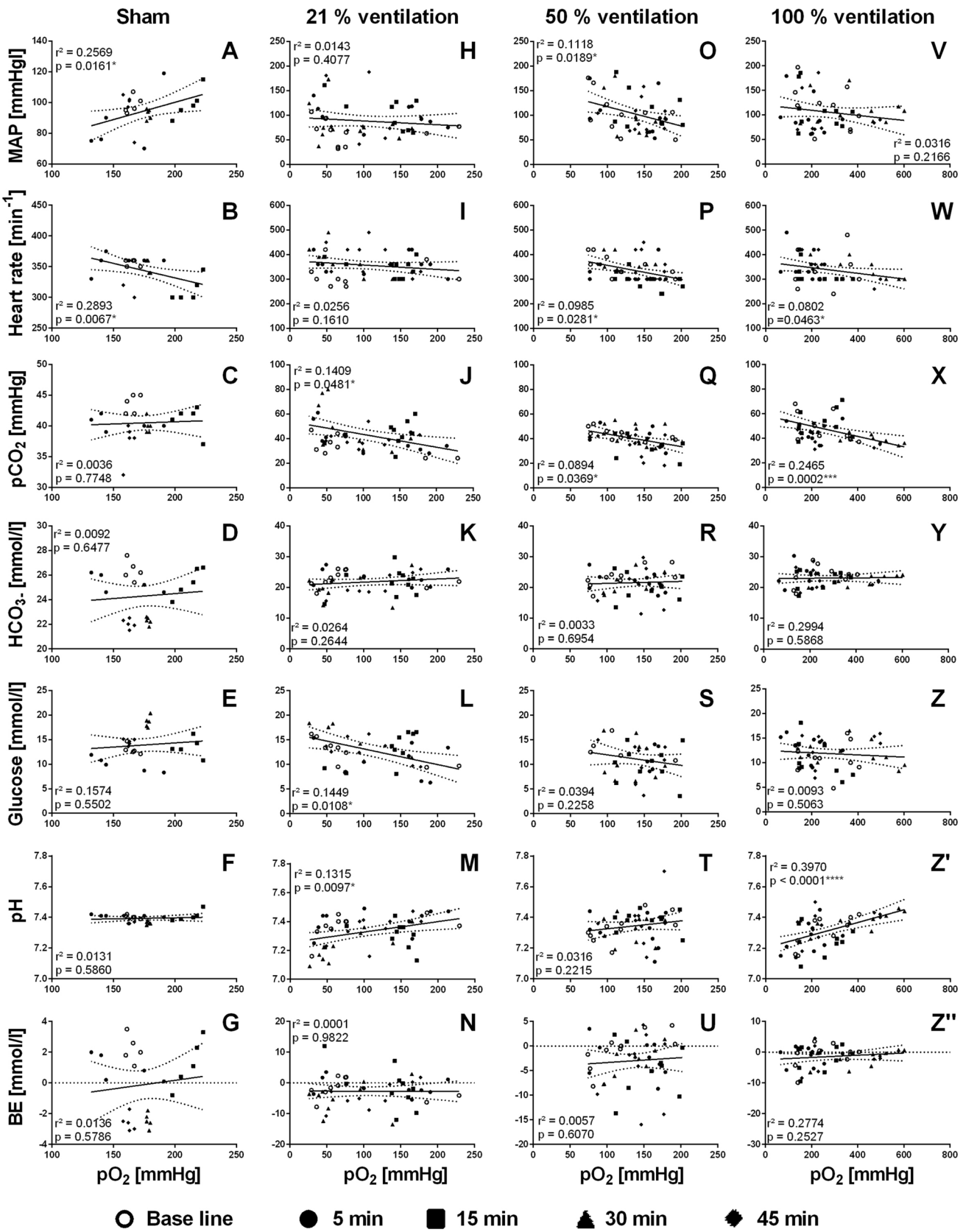
Sham
21 % ventilation
50 % ventilation
100 % ventilation
MAP [mmHgl]
Heart rate [min-1]
pCO2 [mmHg]
HCO3- [mmol/l]
Glucose [mmol/l]
pH
BE [mmol/l]
pO2 [mmHg]
A r² = 0.2569 p = 0.0161*
H r² = 0.0143 p = 0.4077
O r² = 0.1118 p = 0.0189*
V r² = 0.0316 p = 0.2166
B r² = 0.2893 p = 0.0067*
I r² = 0.0256 p = 0.1610
P r² = 0.0985 p = 0.0281*
W r² = 0.0802 p =0.0463*
C r² = 0.0036 p = 0.7748
J r² = 0.1409 p = 0.0481*
Q r² = 0.0894 p = 0.0369*
X r² = 0.2465 p = 0.0002***
D r² = 0.0092 p = 0.6477
K r² = 0.0264 p = 0.2644
R r² = 0.0033 p = 0.6954
Y r² = 0.2994 p = 0.5868
E r² = 0.1574 p = 0.5502
L r² = 0.1449 p = 0.0108*
S r² = 0.0394 p = 0.2258
Z r² = 0.0093 p = 0.5063
F r² = 0.0131 p = 0.5860
M r² = 0.1315 p = 0.0097*
T r² = 0.0316 p = 0.2215
Z' r² = 0.3970 p < 0.0001****
G r² = 0.0136 p = 0.5786
N r² = 0.0001 p = 0.9822
U r² = 0.0057 p = 0.6070
Z'' r² = 0.2774 p = 0.2527
Base line
5 min
15 min
30 min
45 min

◂**Fig. 3** Linear regression analysis of the relationship between the independent variable pO_2 and the dependent variables in the form of vital parameters (VP) using the individual values for each animal within one experimental group. *r* correlation coefficient indicating strength and direction of the linear relationship between pO_2 and the respective VP; positive slope: pO_2 and VP change in the same direction; negative slope: pO_2 and VP change in opposite directions; $^*p < 0.05$; $^{**} < 0.005$; $^{***} < 0.001$; $^{****} < 0.0001$: significant linear dependencies between pO_2 and VP. Please note the different symbols of the data points indicating their affiliation to the time of measurement (BL, 5, 15, 30, and 45 min)

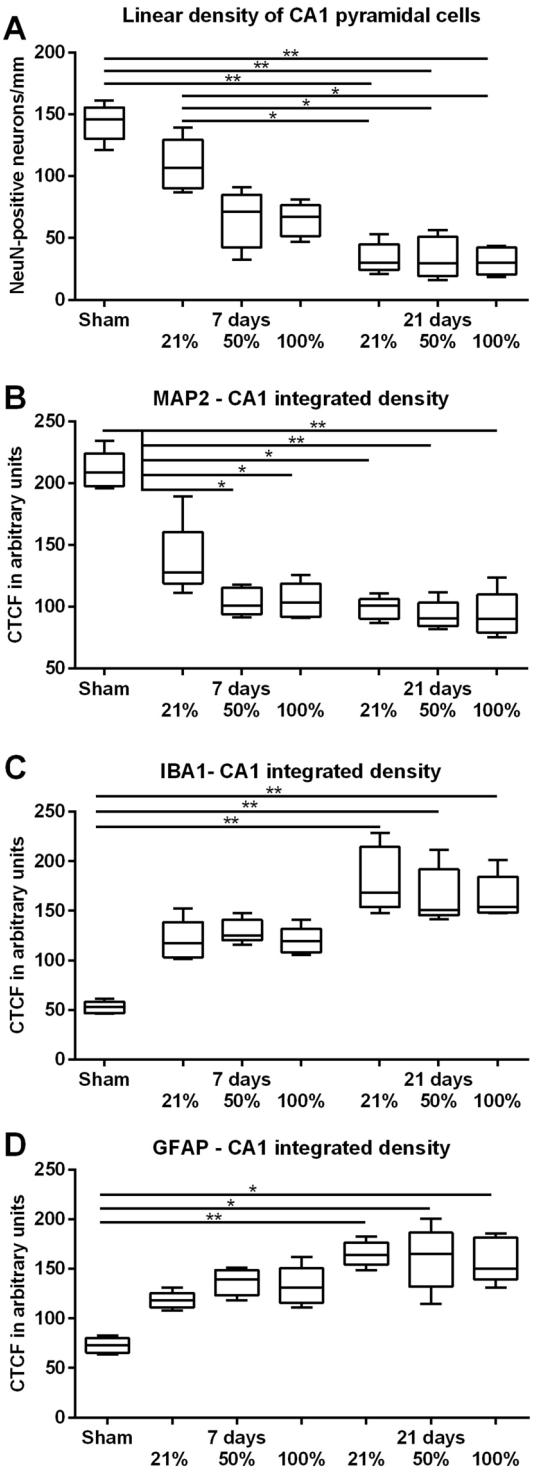

Fig. 4 Statistical analysis of the different stainings. **a** Independent ▸ on the ventilation regime, reduced linear density of NeuN-positive neurons indicated significant neurodegeneration after 21 days. In the short-term survival group, 21% O_2 ventilation showed a significantly lower neurodegeneration pattern (neuroprotective potency), when compared with the longer ST. **b** MAP2 staining indicated early and ventilation-independent neuronal dendrite degeneration. **c** IBA1 staining demonstrated early (tendentially) and long-lasting ventilation-independent microglial activation. **d** GFAP staining indicated a significant ventilation-independent reactive astrogliosis in the long-term survival groups. The integrated densities refer to the complete CA1 region, including Stratum oriens, Stratum pyramidale, Stratum radiatum, and Stratum lacunosum moleculare. Boxplots display the likely and full range of variation from min to max and the median; non-parametric Kruskal–Wallis/Dunn's post-hoc test

patterns despite different recovery times (e.g., rats 16 and 19) and vice versa (e.g., rats 6 and 7, and rats 14 and 15).

Our linear regression analysis of the vital parameters (MAP, heart rate, pO_2, pCO_2, glucose, HCO_3^-, pH, or BE as independent variables) and hippocampal CA1 immunohistology (GFAP, IBA1, and MAP2: integrated density; NeuN: LD as dependent variables) for the different O_2 ventilation regimes at both STs provided only partial, heterogeneous correlations (Table 2, ST 7 days; Table 3, ST 21 days). Thus, the regression analysis indicated that the early post-ROSC phase had only a marginal effect on the histological outcome.

Discussion

Our findings revealed that normoxic (21% O_2) post-ROSC ventilation attenuates hippocampal CA1 degeneration in a rat ACA/R model, but that the attenuation is only temporary. To obtain more practice-relevant evidence, we examined the neuronal and glial cell pattern after STs of 7 and 21 days and found evidence of a neuroprotective effect of normoxic post-ROSC ventilation only in the short-term ST. This neuroprotective effect was disappeared completely after 21 days' ST. ACA/R-induced injury is bi-phasic. It starts with primary injury resulting from the immediate lack of cerebral blood flow after CA. Secondary injury begins immediately after ROSC and lasts for hours and days after ACA/R (Sekhon et al. 2017). Our post-ROSC intervention targeted only the secondary injury processes. One could argue that a study using normoxia already during resuscitation must be more successful because it targets both the primary and the secondary injury. This contention is supported by studies of Hazelton (Hazelton et al. 2010), who found neuroprotective

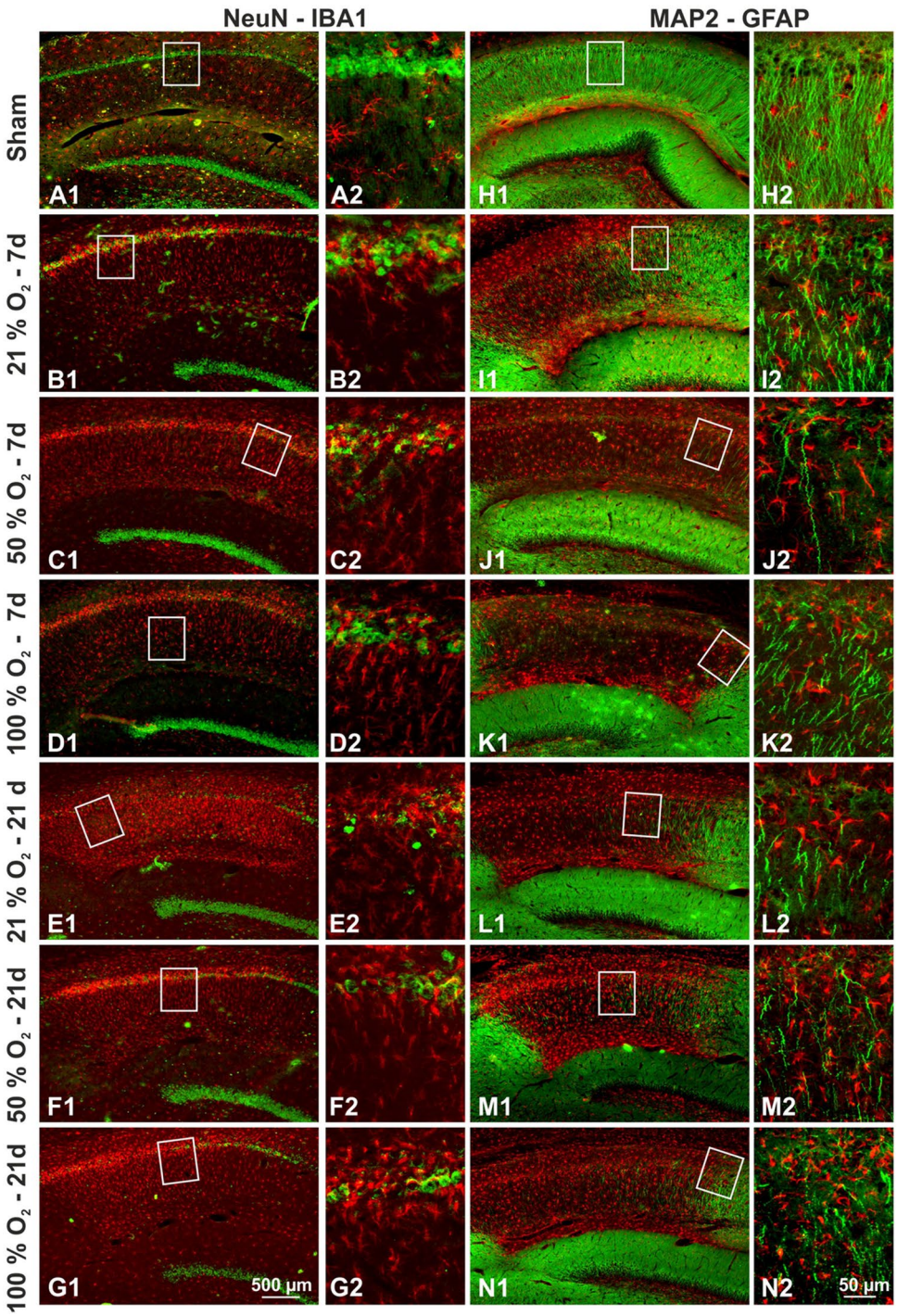

Fig. 5 ACA/R-induced hippocampal CA1 degeneration. **a1**–**g2** Co-immunostaining of neuronal marker NeuN (green) and microglia marker IBA1 (red); **h1**–**n2** Co-immunostaining of neuronal marker MAP2 (green) and astroglial marker GFAP (red). The frames indicate the area of the respective high-magnification images, which were taken from a parallel slice. Scale bar = 500 µm valid for all number 1 pictures, scale bar 50 µm valid for all number 2 pictures

effects of normoxic ventilation after a longer ST of 30 days, whereby normoxia was already used for resuscitation.

However, most of the other studies indicating that reoxygenation with normoxic O_2 reduces mortality (Mickel et al. 1987), delays cellular recovery (Solberg et al. 2010) and lessens neuronal death in the hippocampal CA1 region when compared to ventilation with 100% O_2 (Balan et al. 2006; Vereczki et al. 2006; Solevag et al. 2016) are not suitable for supporting this thesis. This is also true for studies showing similar neuroprotective effects for other brain regions [cerebellum: (Lee et al., 2019); cortex: (Solberg et al. 2012); striatum: (Brucken et al. 2010)]. In these studies, the brains were examined after STs of a few days or even only hours [24 h and shorter: (Balan et al. 2006; Vereczki et al. 2006; Solberg et al. 2010, 2012; Solevag et al. 2016; Lee et al. 2019); between 2 and 7 days: (Brucken et al. 2010)]. Our post-ROSC normoxic ventilation was also neuroprotective in this time window.

Table 2 Linear regression analysis of the relationship between the independent variable (vital parameter) and the dependent variable (MAP2, IBA1, GFAP: integrated density; NeuN: linear density; after 7 days of survival)

Survival time 7 days	Immunohistology of the hippocampal CA1 region											
	NeuN			MAP2			IBA1			GFAP		
Vital parameters	R^2	p	slope	R^2	p	slope	R^2	p	slope	R^2	p	slope
MAP												
21% O_2, 5′	0.3699	n.s	↗	0.3156	n.s	↗	0.3124	n.s	↘	0.2201	n.s	↗
21% O_2, 15′	0.0953	n.s	↘	0.0233	n.s	–	0.7793	*	↘	0.4021	n.s	↗
21% O_2, 30′	0.0298	n.s	↘	0.0609	n.s	↘	0.7497	n.s	↘	0.8417	*	↗
21% O_2, 45′	0.0069	n.s	–	0.0427	n.s	↘	0.8546	*	↘	0.8579	*	↗
50% O_2, 5′	0.3378	n.s	↗	0.1011	n.s	↗	0.0082	n.s	–	0.0331	n.s	↘
50% O_2, 15′	0.2684	n.s	↗	0.0706	n.s	↗	0.4204	n.s	↗	0.2247	n.s	↘
50% O_2, 30′	0.4137	n.s	↗	0.1109	n.s	↗	0.2326	n.s	↗	0.1214	n.s	↘
50% O_2, 45′	0.1437	n.s	↗	0.0000	n.s	–	0.0267	n.s	↘	0.0709	n.s	↗
100% O_2, 5′	0.1784	n.s	↘	0.0002	n.s	–	0.1366	n.s	↘	0.0816	n.s	↗
100% O_2, 15′	0.5620	n.s	↘	0.1816	n.s	↗	0.2924	n.s	↘	0.0077	n.s	–
100% O_2, 30′	0.5856	n.s	↘	0.1924	n.s	↗	0.0913	n.s	↘	0.0338	n.s	↗
100% O_2, 45′	0.4380	n.s	↘	0.0955	n.s	↗	0.0403	n.s	–	0.1249	n.s	↗
Heart rate												
21% O_2, 5′	0.5699	n.s	↗	0.8423	*	↗	0.0473	n.s	↗	0.4854	n.s	↘
21% O_2, 15′	0.0194	n.s	–	0.0858	n.s	↘	0.5416	n.s	↘	0.2439	n.s	↗
21% O_2, 30′	0.1562	n.s	↗	0.0383	n.s	↗	0.7802	*	↘	0.4676	n.s	↗
21% O_2, 45′	0.0245	n.s	–	0.0482	n.s	↘	0.4329	n.s	↘	0.4922	n.s	↗
50% O_2, 5′	0.1852	n.s	↗	0.0025	n.s	–	0.4497	n.s	↗	0.2115	n.s	↘
50% O_2, 15′	0.3137	n.s	↗	0.1316	n.s	↗	0.1304	n.s	↗	0.0421	n.s	↘
50% O_2, 30′	0.7292	n.s	↗	0.2369	n.s	↗	0.1718	n.s	↗	0.1909	n.s	↘
50% O_2, 45′	0.3977	n.s	↗	0.1314	n.s	↗	0.1154	n.s	↗	0.4361	n.s	↘
100% O_2, 5′	0.2627	n.s	↗	0.4860	n.s	↘	0.0371	n.s	↗	0.5045	n.s	↗
100% O_2, 15′	0.1357	n.s	↗	0.0021	n.s	–	0.0813	n.s	↗	0.0412	n.s	↘
100% O_2, 30′	0.5929	n.s	↗	0.2150	n.s	↘	0.3524	n.s	↗	0.0055	n.s	–
100% O_2, 45′	0.6160	n.s	↗	0.2133	n.s	↘	0.3226	n.s	↗	0.1282	n.s	↘
pCO_2												
21% O_2, 5′	0.1019	n.s	↗	0.0131	n.s	–	0.0092	n.s	–	0.0090	n.s	–
21% O_2, 15′	0.1618	n.s	↗	0.0091	n.s	–	0.0121	n.s	–	0.2299	n.s	↗
21% O_2, 30′	0.1982	n.s	↗	0.0060	n.s	–	0.2052	n.s	↗	0.0532	n.s	↘
21% O_2, 45′	0.0981	n.s	↘	0.1026	n.s	↘	0.2357	n.s	↗	0.0066	n.s	–
50% O_2, 5′	0.4377	n.s	↘	0.4748	n.s	↘	0.2285	n.s	↗	0.0197	n.s	–
50% O_2, 15′	0.6822	n.s	↘	0.2813	n.s	↘	0.0000	n.s	–	0.0140	n.s	–
50% O_2, 30′	0.0175	n.s	–	0.3843	n.s	↘	0.3422	n.s	↗	0.1735	n.s	↘
50% O_2, 45′	0.0030	n.s	–	0.2156	n.s	↘	0.7314	n.s	↗	0.3624	n.s	↘
100% O_2, 5′	0.2468	n.s	↗	0.0795	n.s	↘	0.0318	n.s	↘	0.1630	n.s	↗
100% O_2, 15′	0.0000	n.s	–	0.1160	n.s	↘	0.0219	n.s	–	0.5548	n.s	↗
100% O_2, 30′	0.0079	n.s	–	0.1382	n.s	↘	0.1030	n.s	↘	0.5496	n.s	↗
100% O_2, 45′	0.3113	n.s	↘	0.0175	n.s	–	0.3096	n.s	↘	0.0065	n.s	–
Glucose												
21% O_2, 5′	0.0398	n.s	↗	0.2499	n.s	↗	0.0501	n.s	↗	0.6633	n.s	↘
21% O_2, 15′	0.0426	n.s	↘	0.0919	n.s	↘	0.1661	n.s	↗	0.0454	n.s	↗
21% O_2, 30′	0.0920	n.s	↘	0.2548	n.s	↘	0.5830	n.s	↗	0.0218	n.s	–
21% O_2, 45′	0.3760	n.s	↘	0.3364	n.s	↘	0.1935	n.s	↗	0.0103	n.s	–
50% O_2, 5′	0.0094	n.s	–	0.0268	n.s	↗	0.0416	n.s	↘	0.1575	n.s	↗
50% O_2, 15′	0.5202	n.s	↘	0.3130	n.s	↘	0.6078	n.s	↘	0.5578	n.s	↗
50% O_2, 30′	0.0000	n.s	–	0.2921	n.s	↗	0.1698	n.s	↘	0.0377	n.s	↗
50% O_2, 45′	0.1625	n.s	↘	0.0250	n.s	↗	0.3054	n.s	↘	0.2254	n.s	↗

Table 2 (continued)

Survival time 7 days	Immunohistology of the hippocampal CA1 region											
	NeuN			MAP2			IBA1			GFAP		
Vital parameters	R^2	p	slope	R^2	p	slope	R^2	p	slope	R^2	p	slope
100% O_2, 5′	0.2715	n.s	↗	0.2198	n.s	↘	0.5641	n.s	↗	0.1662	n.s	↗
100% O_2, 15′	0.0844	n.s	↗	0.1326	n.s	↘	0.5665	n.s	↗	0.1597	n.s	↗
100% O_2, 30′	0.0032	n.s	–	0.0000	n.s	–	0.0828	n.s	↘	0.9592	**	↗
100% O_2, 45′	0.0791	n.s	↗	0.0101	n.s	–	0.0146	n.s	–	0.4761	n.s	↗
pH												
21% O_2, 5′	0.2763	n.s	↘	0.0050	n.s	–	0.1341	n.s	↗	0.2796	n.s	↘
21% O_2, 15′	0.1810	n.s	↘	0.0041	n.s	–	0.0794	n.s	↗	0.3550	n.s	↘
21% O_2, 30′	0.1045	n.s	↘	0.0314	n.s	–	0.0214	n.s	–	0.3283	n.s	↘
21% O_2, 45′	0.0914	n.s	↘	0.0364	n.s	–	0.0286	n.s	–	0.0634	n.s	–
50% O_2, 5′	0.8502	*	↗	0.5763	n.s	↗	0.0000	n.s	–	0.0124	n.s	–
50% O_2, 15′	0.2591	n.s	↘	0.0641	n.s	–	0.9138	*	↘	0.9054	*	↗
50% O_2, 30′	0.0271	n.s	–	0.0665	n.s	–	0.9124	*	↘	0.6371	n.s	↗
50% O_2, 45′	0.1235	n.s	–	0.0014	n.s	–	0.9505	*	↘	0.9544	*	↗
100% O_2, 5′	0.0197	n.s	–	0.1974	n.s	↗	0.2518	n.s	↘	0.1666	n.s	↗
100% O_2, 15′	0.0004	n.s	–	0.1445	n.s	↗	0.0245	n.s	–	0.2289	n.s	↘
100% O_2, 30′	0.0047	n.s	–	0.1524	n.s	↗	0.0804	n.s	↗	0.4630	n.s	↘
100% O_2, 45′	0.0799	n.s	↗	0.0003	n.s	–	0.4720	n.s	↗	0.1625	n.s	↘
HCO_3												
21% O_2, 5′	0.0344	n.s	–	0.0734	n.s	↘	0.3213	n.s	↗	0.3009	n.s	↘
21% O_2, 15′	0.2219	n.s	↘	0.0000	n.s	–	0.1507	n.s	↗	0.3569	n.s	↘
21% O_2, 30′	0.0540	n.s	↗	0.2684	n.s	↗	0.5783	n.s	↗	0.9180	*	↘
21% O_2, 45′	0.1638	n.s	↘	0.0006	n.s	–	0.0122	n.s	–	0.0433	n.s	↘
50% O_2, 5′	0.8301	*	↗	0.5677	n.s	↗	0.0000	n.s	–	0.0234	n.s	–
50% O_2, 15′	0.5364	n.s	↗	0.2575	n.s	↗	0.1273	n.s	↗	0.0838	n.s	↘
50% O_2, 30′	0.1297	n.s	↘	0.1980	n.s	↘	0.3856	n.s	↘	0.3453	n.s	↗
50% O_2, 45′	0.0571	n.s	↘	0.4541	n.s	↘	0.9137	*	↘	0.0179	n.s	–
100% O_2, 5′	0.2411	n.s	↗	0.0220	n.s	–	0.0102	n.s	–	0.0512	n.s	↗
100% O_2, 15′	0.2335	n.s	↗	0.0430	n.s	–	0.2254	n.s	↗	0.0932	n.s	↗
100% O_2, 30′	0.4450	n.s	↗	0.5170	n.s	↘	0.1003	n.s	↗	0.4230	n.s	↗
100% O_2, 45′	0.2303	n.s	↗	0.1615	n.s	↘	0.5977	n.s	↗	0.6441	n.s	↘
Base excess												
21% O_2, 5′	0.5279	n.s	↘	0.5663	n.s	↘	0.0554	n.s	↘	0.5854	n.s	↗
21% O_2, 15′	0.0815	n.s	↘	0.0002	n.s	–	0.3270	n.s	↗	0.5391	n.s	↘
21% O_2, 30′	0.0598	n.s	↗	0.2283	n.s	↗	0.4762	n.s	↗	0.9674	**	↘
21% O_2, 45′	0.1086	n.s	↘	0.0000	n.s	–	0.0139	n.s	–	0.0409	n.s	↘
50% O_2, 5′	0.2256	n.s	↗	0.3380	n.s	↗	0.1978	n.s	↗	0.0800	n.s	↘
50% O_2, 15′	0.5624	n.s	↗	0.7043	n.s	↗	0.1610	n.s	↗	0.5215	n.s	↗
50% O_2, 30′	0.3377	n.s	↗	0.6961	n.s	↗	0.2989	n.s	↘	0.3196	n.s	↗
50% O_2, 45′	0.2238	n.s	↗	0.0326	n.s	↗	0.0837	n.s	↘	0.0129	n.s	–
100% O_2, 5′	0.2720	n.s	↗	0.0444	n.s	↘	0.0081	n.s	–	0.0998	n.s	↗
100% O_2, 15′	0.4469	n.s	↗	0.2717	n.s	↘	0.6178	n.s	↗	0.0525	n.s	↗
100% O_2, 30′	0.8991	*	↗	0.8543	*	↘	0.1735	n.s	↗	0.0232	n.s	–
100% O_2, 45′	0.0899	n.s	↗	0.1083	n.s	↘	0.2463	n.s	↗	0.7882	*	↘
pO_2												
21% O_2, 5′	0.1344	n.s	↘	0.0033	n.s	–	0.2732	n.s	↘	0.0028	n.s	–
21% O_2, 15′	0.3711	n.s	↘	0.1523	n.s	↘	0.5210	n.s	↘	0.2361	n.s	↗
21% O_2, 30′	0.2061	n.s	↘	0.0417	n.s	–	0.6069	n.s	↘	0.1709	n.s	↗
21% O_2, 45′	0.1446	n.s	↘	0.0017	n.s	–	0.2720	n.s	↘	0.0026	n.s	–

Table 2 (continued)

Survival time 7 days	Immunohistology of the hippocampal CA1 region											
	NeuN			MAP2			IBA1			GFAP		
Vital parameters	R^2	p	slope	R^2	p	slope	R^2	p	slope	R^2	p	slope
50% O_2, 5′	0.6910	n.s	↗	0.2352	n.s	↗	0.1071	n.s	↗	0.3141	n.s	↘
50% O_2, 15′	0.5442	n.s	↗	0.2246	n.s	↗	0.0204	n.s	–	0.0062	n.s	–
50% O_2, 30′	0.0727	n.s	↗	0.3580	n.s	↗	0.0684	n.s	↗	0.1350	n.s	↘
50% O_2, 45′	0.0000	n.s	–	0.0181	n.s	–	0.5315	n.s	↗	0.1899	n.s	↘
100% O_2, 5′	0.8032	*	↗	0.0005	n.s	–	0.3456	n.s	↗	0.5612	n.s	↘
100% O_2, 15′	0.4775	n.s	↗	0.3684	n.s	↗	0.0024	n.s	–	0.1700	n.s	↘
100% O_2, 30′	0.4781	n.s	↗	0.5234	n.s	↗	0.2445	n.s	↘	0.0272	n.s	–
100% O_2, 45′	0.2289	n.s	↗	0.6266	n.s	↗	0.4535	n.s	↘	0.1963	n.s	↗

R^2 correlation coefficient indicating strength and direction of the linear relationship, *positive slope* ↗ both parameter change in the same direction, *negative slope* ↘ parameter change in opposite directions, *slope* – no linear relationship at all

*$p < 0.05$; ** < 0.005; significance of deviation from zero

ACA/R-induced cell death continues for days to weeks and is accompanied by glial reactions (Sugawara et al. 2002). However, in our experiments, the different ventilation regimes had no effect whatsoever on ACA/R-mediated microglial and astroglial activation patterns. This missing glia effect may be one reason for the lack of normoxia-mediated neuroprotection in the long-term survival group. Literature data (Hazelton et al. 2010) support this presumption. They found that microglia activation was reduced by normoxic resuscitation, and they assumed that reduction of early microglia activation may have provided the basis for the demonstrated late (30 days) neuroprotection. However, in our experiments, there was no normoxic-mediated reduction of microglia activation and, thus, no subsequent neuroprotection. But the authors are honest; they admitted that their findings are not sufficient to rule out the reversal: reduced microglial activation as result of reduced neurodegeneration.

In our experiments, microglia were also activated in the long-term survival groups and that even more then in thus with shorter ST. That indicates a reaction of longer-lasting cell (neuronal) death processes. Long-lasting (56 days) ischemia-induced microglial activation was also demonstrated by Sugawara et al. (2002). As we used a relative short CA period (6 min), it was of particular interest to us that in Sugawara et al.'s study the duration of cardiac arrest (5 vs. 10 min) was irrelevant both for microglia activation and for the percentage of CA1 neuronal loss.

Ischemia-mediated activation of microglia as the first step of inflammatory response begins immediately after the insult, lasts for weeks and produces wide-ranging and very complex neuroprotective as well as neurodegenerative processes (Benakis et al. 2014; Guruswamy and ElAli 2017; Jin et al. 2017; Kronenberg et al. 2018). Along with neutrophils and macrophages activated microglia infiltrate the infarct area immediately following ACA/R-mediated injury and contribute to the upregulated expression of pro-inflammators, such as inducible nitric oxide synthase (iNOS), NO, interleukins (e.g. IL-6, IL-8), interferon-Ɣ, matrix metalloproteinase 9, and either tumor necrosis factor α or IL-1β, mediating neuronal death and infarct expansion (Ma et al. 2017; Gulke et al. 2018; Lambertsen et al. 2019; Qin et al. 2019). However, with these damaging effects, microglia also laid the foundation for subsequent neuronal regeneration, which could not happen without cell debris being eliminated (Neumann et al. 2009). And, being also an endogenous pool of neurotrophic factors, such as IGF-1, GDNF, BDNF, and VEGF, in addition to anti-inflammatory cytokines such as TGF-β, activated microglia can be neuroprotective per se (Lalancette-Hebert et al. 2007; Narantuya et al. 2010; Ma et al. 2017).

Moreover, microglia are subject to the ischemic cascade, including ATP depletion and Na^+/K^+ pump failure, with subsequent mitochondrial damage (Gong et al. 2018) and cell fragmentation (Lambertsen et al. 2019; Zhang 2019). As shown in cell cultures, these individual reactions of microglia were induced directly by the initial lack of oxygen (Widmer et al. 2007). In vivo, reduction of blood flow and the consequent lack of oxygen supply decreased significantly the retracting/extending process activity of microglia (Masuda et al. 2011), whereby these morphological transformations were arrested by the complete loss of blood flow. That might explain, at least partly, the different results when comparing CA models with carotid occlusion models.

As anticipated we showed ongoing activation of astroglia after 21 days' ST. However, as with microglia, there was no effect of the various O_2 ventilation regimes. Reactive gliosis is a direct consequence of neurodegeneration (Revuelta et al. 2019). As we found no ventilation-dependent differences in the neurodegeneration pattern after 21 days' ST, only limited respective differences in astroglia responses could be

Table 3 Linear regression analysis of the relationship between the independent variable (vital parameter) and the dependent variable (MAP2, IBA1, GFAP: integrated density; NeuN: linear density; after 21 days of survival)

Survival time 21 days	Immunohistology of the hippocampal CA1 region											
	NeuN			MAP2			IBA1			GFAP		
Vital parameters	R^2	p	slope	R^2	p	slope	R^2	p	slope	R^2	p	slope
MAP												
21% O_2, 5′	0.8534	*	↗	0.8040	*	↘	0.4923	n.s	↘	0.5517	n.s	↘
21% O_2, 15′	0.1795	n.s	↘	0.0190	n.s	–	0.1341	n.s	↗	0.0528	n.s	↘
21% O_2, 30′	0.4109	n.s	↘	0.0594	n.s	↗	0.1883	n.s	↗	0.0244	n.s	–
21% O_2, 45′	0.2670	n.s	↘	0.0009	n.s	–	0.0861	n.s	↗	0.1208	n.s	↘
50% O_2, 5′	0.5872	n.s	↘	0.4454	n.s	↗	0.0002	n.s	–	0.0301	n.s	↗
50% O_2, 15′	0.3674	n.s	↗	0.0561	n.s	↘	0.2138	n.s	↘	0.0114	n.s	–
50% O_2, 30′	0.6451	n.s	↗	0.0483	n.s	↘	0.5922	n.s	↘	0.1597	n.s	↘
50% O_2, 45′	0.5545	n.s	↗	0.0104	n.s	–	0.4684	n.s	↘	0.1608	n.s	↗
100% O_2, 5′	0.0073	n.s	–	0.0178	n.s	–	0.1007	n.s	↗	0.3705	n.s	↗
100% O_2, 15′	0.0005	n.s	–	0.0395	n.s	↗	0.0063	n.s	–	0.1880	n.s	↗
100% O_2, 30′	0.0000	n.s	–	0.0217	n.s	–	0.0174	n.s	–	0.4542	n.s	↗
100% O_2, 45′	0.0036	n.s	–	0.0667	n.s	↘	0.0017	n.s	–	0.6677	n.s	↗
Heart rate												
21% O_2, 5′	0.6857	n.s	↗	0.9223	**	↘	0.6354	n.s	↘	0.7372	n.s	↘
21% O_2, 15′	0.5941	n.s	↗	0.4521	n.s	↘	0.4197	n.s	↘	0.2797	n.s	↘
21% O_2, 30′	0.6217	n.s	↗	0.5657	n.s	↘	0.3783	n.s	↘	0.4378	n.s	↘
21% O_2, 45′	0.5845	n.s	↗	0.1902	n.s	↘	0.0978	n.s	↘	0.0803	n.s	↘
50% O_2, 5′	0.6665	n.s	↘	0.3169	n.s	↗	0.0687	n.s	↗	0.0093	n.s	–
50% O_2, 15′	0.6508	n.s	↘	0.0302	n.s	–	0.2442	n.s	↗	0.5719	n.s	↗
50% O_2, 30′	0.3901	n.s	↘	0.0030	n.s	–	0.1834	n.s	↗	0.0869	n.s	↗
50% O_2, 45′	0.1045	n.s	↘	0.0036	n.s	–	0.0374	n.s	↗	0.0024	n.s	–
100% O_2, 5′	0.1785	n.s	↗	0.2860	n.s	↘	0.0135	n.s	–	0.6616	n.s	↗
100% O_2, 15′	0.2081	n.s	↗	0.0000	n.s	–	0.0967	n.s	↗	0.3550	n.s	↗
100% O_2, 30′	0.1443	n.s	↗	0.1235	n.s	↘	0.3177	n.s	↗	0.8726	*	↗
100% O_2, 45′	0.0254	n.s	–	0.5448	n.s	↗	0.0013	n.s	–	0.7449	n.s	↘
pCO_2												
21% O_2, 5′	0.0967	n.s	↘	0.6909	n.s	↘	0.6106	n.s	↘	0.7026	n.s	↘
21% O_2, 15′	0.1181	n.s	↘	0.0756	n.s	↘	0.1280	n.s	↘	0.3108	n.s	↘
21% O_2, 30′	0.3266	n.s	↘	0.0268	n.s	↗	0.0944	n.s	↘	0.8117	n.s	↘
21% O_2, 45′	0.8474	n.s	*	0.8241	*	↗	0.6586	n.s	↗	0.4302	n.s	↗
50% O_2, 5′	0.2918	n.s	↘	0.8188	*	↗	0.0736	n.s	↗	0.1108	n.s	↘
50% O_2, 15′	0.1486	n.s	↘	0.6530	n.s	↗	0.1452	n.s	↗	0.1498	n.s	↘
50% O_2, 30′	0.2523	n.s	↘	0.7918	*	↗	0.1000	n.s	↗	0.1163	n.s	↘
50% O_2, 45′	0.5084	n.s	↘	0.4976	n.s	↗	0.0940	n.s	↗	0.0117	n.s	–
100% O_2, 5′	0.2133	n.s	↗	0.4544	n.s	↘	0.3496	n.s	↘	0.3212	n.s	↘
100% O_2, 15′	0.0089	n.s	–	0.7855	*	↘	0.3690	n.s	↘	0.0438	n.s	↘
100% O_2, 30′	0.1928	n.s	↗	0.5065	n.s	↘	0.4562	n.s	↘	0.0414	n.s	–
100% O_2, 45′	0.2649	n.s	↗	0.3700	n.s	↘	0.5752	n.s	↘	0.0004	n.s	–
Glucose												
21% O_2, 5′	0.3359	n.s	↗	0.0249	n.s	–	0.1625	n.s	↘	0.4666	n.s	↘
21% O_2, 15′	0.0710	n.s	↗	0.0069	n.s	–	0.3428	n.s	↗	0.0024	n.s	–
21% O_2, 30′	0.1133	n.s	↗	0.0003	n.s	–	0.0022	n.s	–	0.0015	n.s	–
21% O_2, 45′	0.1177	n.s	↗	0.0119	n.s	–	0.3156	n.s	↘	0.0662	n.s	↘
50% O_2, 5′	0.7787	*	↘	0.0000	n.s	–	0.1520	n.s	↗	0.6198	n.s	↗
50% O_2, 15′	0.0046	n.s	–	0.1417	n.s	↘	0.0000	n.s	–	0.0090	n.s	–
50% O_2, 30′	0.0128	n.s	–	0.7076	n.s	↘	0.1665	n.s	↗	0.4947	n.s	↗
50% O_2, 45′	0.0000	n.s	–	0.5201	n.s	↘	0.1384	n.s	↗	0.1772	n.s	↗

Table 3 (continued)

Survival time 21 days	Immunohistology of the hippocampal CA1 region											
	NeuN			MAP2			IBA1			GFAP		
Vital parameters	R^2	p	slope	R^2	p	slope	R^2	p	slope	R^2	p	slope
100% O_2, 5′	0.0775	n.s	↗	0.7154	n.s	↗	0.1174	n.s	↘	0.4777	n.s	↘
100% O_2, 15′	0.0116	n.s	–	0.6848	n.s	↘	0.4742	n.s	↘	0.0492	n.s	↗
100% O_2, 30′	0.1261	n.s	↘	0.5639	n.s	↘	0.1646	n.s	↘	0.0008	n.s	–
100% O_2, 45′	0.1841	n.s	↘	0.4796	n.s	↘	0.1013	n.s	↘	0.0004	n.s	–
pH												
21% O_2, 5′	0.2850	n.s	↘	0.6661	n.s	↘	0.9945	***	↗	0.4319	n.s	↗
21% O_2, 15′	0.0080	n.s	–	0.2325	n.s	↘	0.6459	n.s	↗	0.1327	n.s	↗
21% O_2, 30′	0.1741	n.s	↘	0.2644	n.s	↗	0.6735	n.s	↗	0.0581	n.s	↗
21% O_2, 45′	0.0560	n.s	–	0.3173	n.s	↘	0.0191	n.s	–	0.4904	n.s	↘
50% O_2, 5′	0.0043	n.s	–	0.2448	n.s	↘	0.1127	n.s	–	0.3028	n.s	↗
50% O_2, 15′	0.2329	n.s	↗	0.6763	n.s	↘	0.1816	n.s	↘	0.0886	n.s	↗
50% O_2, 30′	0.4250	n.s	↗	0.7958	*	↘	0.1336	n.s	↘	0.0206	n.s	–
50% O_2, 45′	0.6186	n.s	↗	0.6076	n.s	↘	0.2719	n.s	↘	0.0023	n.s	–
100% O_2, 5′	0.2133	n.s	↗	0.4544	n.s	↘	0.3496	n.s	↘	0.1849	n.s	↗
100% O_2, 15′	0.0089	n.s	–	0.7855	*	↘	0.3690	n.s	↘	0.1665	n.s	↗
100% O_2, 30′	0.1928	n.s	↗	0.5065	n.s	↘	0.4562	n.s	↘	0.0763	n.s	↗
100% O_2, 45′	0.2649	n.s	↗	0.3700	n.s	↘	0.5752	n.s	↘	0.0251	n.s	↗
HCO_3												
21% O_2, 5′	0.1551	n.s	↘	0.4654	n.s	↗	0.9087	*	↗	0.3104	n.s	↘
21% O_2, 15′	0.2663	n.s	↗	0.5644	n.s	↘	0.6801	n.s	↘	0.6118	n.s	↘
21% O_2, 30′	0.4305	n.s	↘	0.0671	n.s	↗	0.0118	n.s	–	0.0205	n.s	–
21% O_2, 45′	0.7999	*	↘	0.3514	n.s	↗	0.2037	n.s	↗	0.1559	n.s	↗
50% O_2, 5′	0.3011	n.s	↗	0.0983	n.s	↗	0.1260	n.s	↘	0.0340	n.s	–
50% O_2, 15′	0.0040	n.s	↗	0.1702	n.s	↘	0.5291	n.s	↗	0.0462	n.s	↗
50% O_2, 30′	0.0323	n.s	↘	0.0815	n.s	↘	0.6460	n.s	↗	0.0789	n.s	↗
50% O_2, 45′	0.1761	n.s	↘	0.0772	n.s	↗	0.3769	n.s	↗	0.0025	n.s	–
100% O_2, 5′	0.0013	n.s	–	0.6133	n.s	↘	0.0851	n.s	↘	0.6651	n.s	↗
100% O_2, 15′	0.0116	n.s	–	0.2507	n.s	↘	0.1541	n.s	↘	0.4780	n.s	↗
100% O_2, 30′	0.4764	n.s	↗	0.0675	n.s	↘	0.1926	n.s	↘	0.1432	n.s	↗
100% O_2, 45′	0.0239	n.s	↗	0.0042	n.s	–	0.4081	n.s	↗	0.4261	n.s	↗
Base excess												
21% O_2, 5′	0.2977	n.s	↘	0.4283	n.s	↗	0.8666	*	↗	0.1795	n.s	↗
21% O_2, 15′	0.0039	n.s	–	0.1885	n.s	↘	0.2621	n.s	↘	0.4047	n.s	↘
21% O_2, 30′	0.6882	n.s	↘	0.1561	n.s	↗	0.0712	n.s	↗	0.0331	n.s	↗
21% O_2, 45′	0.7727	*	↘	0.2256	n.s	↗	0.1598	n.s	↗	0.0491	n.s	↗
50% O_2, 5′	0.5741	n.s	↘	0.0493	n.s	–	0.0018	n.s	–	0.2151	n.s	↗
50% O_2, 15′	0.0091	n.s	–	0.5445	n.s	↘	0.0678	n.s	↗	0.1123	n.s	↗
50% O_2, 30′	0.2244	n.s	↘	0.0002	n.s	–	0.8144	*	↗	0.0973	n.s	↗
50% O_2, 45′	0.4310	n.s	↘	0.3690	n.s	↗	0.3662	n.s	↗	0.0014	n.s	–
100% O_2, 5′	0.0147	n.s	–	0.5771	n.s	↘	0.0047	n.s	–	0.8561	*	↗
100% O_2, 15′	0.1181	n.s	↘	0.7101	n.s	↘	0.0642	n.s	↘	0.6290	n.s	↗
100% O_2, 30′	0.5100	n.s	↗	0.1267	n.s	↘	0.0171	n.s	–	0.2080	n.s	↗
100% O_2, 45′	0.5613	n.s	↗	0.0244	n.s	–	0.0113	n.s	–	0.0856	n.s	↗
pO_2												
21% O_2, 5′	0.0133	n.s	–	0.0079	n.s	–	0.3198	n.s	↘	0.0122	n.s	–
21% O_2, 15′	0.0204	n.s	–	0.0004	n.s	–	0.2470	n.s	↘	0.0179	n.s	–
21% O_2, 30′	0.0423	n.s	–	0.0612	n.s	↘	0.4656	n.s	↘	0.0048	n.s	–
21% O_2, 45′	0.0073	n.s	–	0.0524	n.s	↘	0.4724	n.s	↘	0.0282	n.s	–

Table 3 (continued)

Survival time 21 days	Immunohistology of the hippocampal CA1 region											
	NeuN			MAP2			IBA1			GFAP		
Vital parameters	R^2	p	slope	R^2	p	slope	R^2	p	slope	R^2	p	slope
50% O_2, 5′	0.4623	n.s	↘	0.6311	n.s	↗	0.1792	n.s	↗	0.0027	n.s	–
50% O_2, 15′	0.7286	n.s	↘	0.3048	n.s	↗	0.2135	n.s	↗	0.1818	n.s	↗
50% O_2, 30′	0.0271	n.s	–	0.1756	n.s	↗	0.0525	n.s	↘	0.0022	n.s	–
50% O_2, 45′	0.0080	n.s	–	0.2038	n.s	↗	0.0018	n.s	–	0.0005	n.s	–
100% O_2, 5′	0.3186	n.s	↗	0.1683	n.s	↘	0.4746	n.s	↘	0.0940	n.s	↗
100% O_2, 15′	0.1463	n.s	↗	0.3312	n.s	↘	0.6926	n.s	↘	0.0118	n.s	–
100% O_2, 30′	0.4218	n.s	↗	0.0745	n.s	↘	0.7186	n.s	↘	0.1153	n.s	↘
100% O_2, 45′	0.3548	n.s	↗	0.0197	n.s	–	0.8655	*	↘	0.1890	n.s	↘

R^2 correlation coefficient indicating strength and direction of the linear relationship, *positive slope* ↗ both parameter change in the same direction, *negative slope* ↘ parameter change in opposite directions, *slope* – no linear relationship at all

*$p < 0.05$; ** < 0.005; significance of deviation from zero

expected. As the astroglia cells are quite robust to ischemia/reperfusion, they are affected less (Shih and Robinson 2018). The authors believe that the mitochondria, particularly the dynamic astrocytic mitochondrial network, are responsible for this resilience. They believe that the dynamic remodeling of the mitochondrial network provides an adaptive mechanism to maintain mitochondrial and, ultimately, astroglial functionality in the setting of ischemia. Against this background, the authors further suggest that astrocytes in the ischemic brain could be a continuous source of energy substrate to neighboring neurons via the lactate shuttle and may also rescue neurons from ischemic injury through donating functional mitochondria (Hayakawa et al. 2016). Moreover, ischemia-stressed astrocytes can be neuroprotective by supplying anti-inflammatory mediators, neurotrophic (Ziemka-Nalecz et al. 2017), and/or vasoactive (Shih and Robinson 2018) factors. However, as with microglia, astroglial cells play dual and opposite roles in ischemia/reperfusion processes, as they may also produce pro-inflammatory and neurotoxic substances such as cytokines or iNOS, thus contributing to neuronal cell death (Rossi et al. 2007; Hailer 2008).

The contention that normoxia already during resuscitation should be more neuroprotective because it targets both primary and secondary injury leads inevitably to the question of whether the current European Resuscitation Guidelines [ventilation during resuscitation with 100% O_2 (Soar et al. 2015)] are up to date. More basic science and clinical research is required to answer this question, as there are also serious objections. There is evidence that using 100% oxygen during resuscitation activates antioxidant enzymes such as superoxide dismutase, catalase, and glutathione peroxidase (Vento et al. 2002; Torres-Cuevas et al. 2017). It is clear that activation of antioxidant enzymes is an expression of oxidative stress. However, it also indicates that cells both can and will defend themselves. Interestingly, the activities of the antioxidant enzymes show positive correlation with pO_2 (Vento et al. 2002). This suggests both normoxia and hyperoxia have detrimental as well as protective effects, thus limiting the superiority of either regime. This interpretation is supported by the findings of Temesvari et al. (2001), showing that there was no significant difference in cerebral histopathology after reoxygenation with either room air or with 100% O_2 following pneumothorax-induced asphyxia. Our results concerning a missing correlation between vital parameters and the hippocampal CA1 neurodegenerative pattern, confirming that the early post-ROSC phase has only a marginal impact of on the histological outcome, fit in well.

As we have mentioned in the Introduction, we extended the focus on the individual heterogeneity of test rats after ACA/R. There is consensus that the great heterogeneity of ACA/R models makes it difficult to compare results and reasoning. Our findings both support this and confirm that the great individual heterogeneity of laboratory animals is a further variable to be considered in ACA/R animal models and their interpretation.

Conclusions

Our findings have shown that that normoxic (21% O_2) post-ROSC ventilation attenuates hippocampal CA1 degeneration in a 6-min asphyxia cardiac arrest/reperfusion rat model, albeit only temporarily, after 7 days' survival time (ST). This neuroprotective effect disappeared completely after 21 days' ST. We assume that this limitation is due to the post-ROSC intervention targeting only processes of the ischemia-induced secondary injury. Our concreted findings show that the different post-ROSC ventilation regimes had no effect on microglial activation, reduction of which is accepted as neuroprotective and induced directly by the

initial lack of oxygen. Furthermore, there was no ventilation-dependent effect on astroglial activation. Astroglia were robust to ischemia/reperfusion and appeared to increase neurons' resistance to ischemia/reperfusion injury through many regulatory opportunities. Consequently, lack of astroglial response should entail a lack in neuronal response.

The limited neuroprotective potency of normoxic post-ROSC ventilation should be remembered when using normoxia clinically. It could be one explanation for the highly variable and all too often unsatisfying functional outcome. And it calls for further experiments to optimize the intervention protocols. Moreover, this study verifies the limited comparability of animal studies because of the individual heterogeneity of the animals used and the experimental regimes.

Acknowledgements The technical assistance provided by Leona Bück and Stefanie Holze is gratefully acknowledged.

Funding None.

Compliance with ethical standards

Conflict of interest All authors claim no conflict of interest.

Ethical approval This study was granted according to the requirements of the German Animal Welfare Act on the Use of Experimental Animals and the Animal Care and Use Committees of Saxony-Anhalt (Permit Number 42502-2-2-947 Uni MD).

References

Balan IS, Fiskum G, Hazelton J, Cotto-Cumba C, Rosenthal RE (2006) Oximetry-guided reoxygenation improves neurological outcome after experimental cardiac arrest. Stroke 37:3008–3013. https://doi.org/10.1161/01.STR.0000248455.73785.b1

Benakis C, Garcia-Bonilla L, Iadecola C, Anrather J (2014) The role of microglia and myeloid immune cells in acute cerebral ischemia. Front Cell Neurosci 8:461. https://doi.org/10.3389/fncel.2014.00461

Brucken A, Kaab AB, Kottmann K, Rossaint R, Nolte KW, Weis J, Fries M (2010) Reducing the duration of 100% oxygen ventilation in the early reperfusion period after cardiopulmonary resuscitation decreases striatal brain damage. Resuscitation 81:1698–1703. https://doi.org/10.1016/j.resuscitation.2010.06.027

Francis A, Baynosa R (2017) Ischaemia-reperfusion injury and hyperbaric oxygen pathways: a review of cellular mechanisms. Diving Hyperb Med 47:110–117

Gong Z, Pan J, Shen Q, Li M, Peng Y (2018) Mitochondrial dysfunction induces NLRP3 inflammasome activation during cerebral ischemia/reperfusion injury. J Neuroinflamm 15:242. https://doi.org/10.1186/s12974-018-1282-6

Gulke E, Gelderblom M, Magnus T (2018) Danger signals in stroke and their role on microglia activation after ischemia. Ther Adv Neurol Disord 11:1756286418774254. https://doi.org/10.1177/1756286418774254

Guruswamy R, ElAli A (2017) Complex roles of microglial cells in ischemic stroke pathobiology: new insights and future directions. Int J Mol Sci. https://doi.org/10.3390/ijms18030496

Hailer NP (2008) Immunosuppression after traumatic or ischemic CNS damage: it is neuroprotective and illuminates the role of microglial cells. Prog Neurobiol 84:211–233. https://doi.org/10.1016/j.pneurobio.2007.12.001

Hayakawa K, Esposito E, Wang X et al (2016) Transfer of mitochondria from astrocytes to neurons after stroke. Nature 535:551–555. https://doi.org/10.1038/nature18928

Hazelton JL, Balan I, Elmer GI et al (2010) Hyperoxic reperfusion after global cerebral ischemia promotes inflammation and long-term hippocampal neuronal death. J Neurotrauma 27:753–762. https://doi.org/10.1089/neu.2009.1186

Jin Y, Wang R, Yang S, Zhang X, Dai J (2017) Role of microglia autophagy in microglia activation after traumatic brain injury. World Neurosurg 100:351–360. https://doi.org/10.1016/j.wneu.2017.01.033

Kronenberg G, Uhlemann R, Richter N et al (2018) Distinguishing features of microglia- and monocyte-derived macrophages after stroke. Acta Neuropathol 135:551–568. https://doi.org/10.1007/s00401-017-1795-6

Lalancette-Hebert M, Gowing G, Simard A, Weng YC, Kriz J (2007) Selective ablation of proliferating microglial cells exacerbates ischemic injury in the brain. J Neurosci 27:2596–2605. https://doi.org/10.1523/JNEUROSCI.5360-06.2007

Lambertsen KL, Finsen B, Clausen BH (2019) Post-stroke inflammation-target or tool for therapy? Acta Neuropathol 137:693–714. https://doi.org/10.1007/s00401-018-1930-z

Lee D, Pearson T, Proctor JL, Rosenthal RE, Fiskum G (2019) Oximetry-Guided normoxic resuscitation following canine cardiac arrest reduces cerebellar Purkinje neuronal damage. Resuscitation 140:23–28. https://doi.org/10.1016/j.resuscitation.2019.04.043

Liu Y, Rosenthal RE, Haywood Y, Miljkovic-Lolic M, Vanderhoek JY, Fiskum G (1998) Normoxic ventilation after cardiac arrest reduces oxidation of brain lipids and improves neurological outcome. Stroke 29:1679–1686. https://doi.org/10.1161/01.str.29.8.1679

Louis ED, Babij R, Lee M, Cortes E, Vonsattel JP (2013) Quantification of cerebellar hemispheric purkinje cell linear density: 32 ET cases versus 16 controls. Mov Disord 28:1854–1859. https://doi.org/10.1002/mds.25629

Ma Y, Wang J, Wang Y, Yang GY (2017) The biphasic function of microglia in ischemic stroke. Prog Neurobiol 157:247–272. https://doi.org/10.1016/j.pneurobio.2016.01.005

Marsala J, Marsala M, Vanicky I, Galik J, Orendacova J (1992) Post cardiac arrest hyperoxic resuscitation enhances neuronal vulnerability of the respiratory rhythm generator and some brainstem and spinal cord neuronal pools in the dog. Neurosci Lett 146:121–124. https://doi.org/10.1016/0304-3940(92)90058-f

Masuda T, Croom D, Hida H, Kirov SA (2011) Capillary blood flow around microglial somata determines dynamics of microglial processes in ischemic conditions. Glia 59:1744–1753. https://doi.org/10.1002/glia.21220

Mickel HS, Vaishnav YN, Kempski O, von Lubitz D, Weiss JF, Feuerstein G (1987) Breathing 100% oxygen after global brain ischemia in Mongolian Gerbils results in increased lipid peroxidation and increased mortality. Stroke 18:426–430. https://doi.org/10.1161/01.str.18.2.426

Narantuya D, Nagai A, Sheikh AM, Masuda J, Kobayashi S, Yamaguchi S, Kim SU (2010) Human microglia transplanted in rat focal ischemia brain induce neuroprotection and behavioral improvement. PLoS ONE 5:e11746. https://doi.org/10.1371/journal.pone.0011746

Neumann H, Kotter MR, Franklin RJ (2009) Debris clearance by microglia: an essential link between degeneration and regeneration. Brain 132:288–295. https://doi.org/10.1093/brain/awn109

Patel JK, Kataya A, Parikh PB (2018) Association between intra- and post-arrest hyperoxia on mortality in adults with cardiac arrest: A systematic review and meta-analysis. Resuscitation 127:83–88. https://doi.org/10.1016/j.resuscitation.2018.04.008

Qin C, Zhou LQ, Ma XT et al (2019) Dual functions of microglia in ischemic stroke. Neurosci Bull 35:921–933. https://doi.org/10.1007/s12264-019-00388-3

Revuelta M, Elicegui A, Moreno-Cugnon L, Buhrer C, Matheu A, Schmitz T (2019) Ischemic stroke in neonatal and adult astrocytes. Mech Ageing Dev 183:111147. https://doi.org/10.1016/j.mad.2019.111147

Rossi DJ, Brady JD, Mohr C (2007) Astrocyte metabolism and signaling during brain ischemia. Nat Neurosci 10:1377–1386. https://doi.org/10.1038/nn2004

Sekhon MS, Ainslie PN, Griesdale DE (2017) Clinical pathophysiology of hypoxic ischemic brain injury after cardiac arrest: a "two-hit" model. Crit Care 21:90. https://doi.org/10.1186/s13054-017-1670-9

Shih EK, Robinson MB (2018) Role of astrocytic mitochondria in limiting ischemic brain injury? Physiology (Bethesda) 33:99–112. https://doi.org/10.1152/physiol.00038.2017

Soar J, Nolan JP, Bottiger BW et al (2015) European Resuscitation Council Guidelines for Resuscitation 2015: section 3. Adult advanced life support. Resuscitation 95:100–147. https://doi.org/10.1016/j.resuscitation.2015.07.016

Solberg R, Enot D, Deigner HP, Koal T, Scholl-Burgi S, Saugstad OD, Keller M (2010) Metabolomic analyses of plasma reveals new insights into asphyxia and resuscitation in pigs. PLoS ONE 5:e9606. https://doi.org/10.1371/journal.pone.0009606

Solberg R, Longini M, Proietti F, Vezzosi P, Saugstad OD, Buonocore G (2012) Resuscitation with supplementary oxygen induces oxidative injury in the cerebral cortex. Free Radic Biol Med 53:1061–1067. https://doi.org/10.1016/j.freeradbiomed.2012.07.022

Solevag AL, Dannevig I, Nakstad B, Saugstad OD (2010) Resuscitation of severely asphyctic newborn pigs with cardiac arrest by using 21% or 100% oxygen. Neonatology 98:64–72. https://doi.org/10.1159/000275560

Solevag AL, Schmolzer GM, O'Reilly M et al (2016) Myocardial perfusion and oxidative stress after 21% vs. 100% oxygen ventilation and uninterrupted chest compressions in severely asphyxiated piglets. Resuscitation 106:7–13. https://doi.org/10.1016/j.resuscitation.2016.06.014

Sugawara T, Lewen A, Noshita N, Gasche Y, Chan PH (2002) Effects of global ischemia duration on neuronal, astroglial, oligodendroglial, and microglial reactions in the vulnerable hippocampal CA1 subregion in rats. J Neurotrauma 19:85–98. https://doi.org/10.1089/089771502753460268

Temesvari P, Karg E, Bodi I et al (2001) Impaired early neurologic outcome in newborn piglets reoxygenated with 100% oxygen compared with room air after pneumothorax-induced asphyxia. Pediatr Res 49:812–819. https://doi.org/10.1203/00006450-200106000-00017

Torres-Cuevas I, Parra-Llorca A, Sanchez-Illana A et al (2017) Oxygen and oxidative stress in the perinatal period. Redox Biol 12:674–681. https://doi.org/10.1016/j.redox.2017.03.011

Vento M, Asensi M, Sastre J, Lloret A, Garcia-Sala F, Minana JB, Vina J (2002) Hyperoxemia caused by resuscitation with pure oxygen may alter intracellular redox status by increasing oxidized glutathione in asphyxiated newly born infants. Semin Perinatol 26:406–410

Vereczki V, Martin E, Rosenthal RE, Hof PR, Hoffman GE, Fiskum G (2006) Normoxic resuscitation after cardiac arrest protects against hippocampal oxidative stress, metabolic dysfunction, and neuronal death. J Cereb Blood Flow Metab 26:821–835. https://doi.org/10.1038/sj.jcbfm.9600234

Vognsen M, Fabian-Jessing BK, Secher N, Lofgren B, Dezfulian C, Andersen LW, Granfeldt A (2017) Contemporary animal models of cardiac arrest: a systematic review. Resuscitation 113:115–123. https://doi.org/10.1016/j.resuscitation.2017.01.024

Walson KH, Tang M, Glumac A et al (2011) Normoxic versus hyperoxic resuscitation in pediatric asphyxial cardiac arrest: effects on oxidative stress. Crit Care Med 39:335–343. https://doi.org/10.1097/CCM.0b013e3181ffda0e

Widmer R, Engels M, Voss P, Grune T (2007) Postanoxic damage of microglial cells is mediated by xanthine oxidase and cyclooxygenase. Free Radic Res 41:145–152. https://doi.org/10.1080/10715760600978807

Young P, Bailey M, Bellomo R et al (2014) HyperOxic Therapy OR NormOxic Therapy after out-of-hospital cardiac arrest (HOT OR NOT): a randomised controlled feasibility trial. Resuscitation 85:1686–1691. https://doi.org/10.1016/j.resuscitation.2014.09.011

Zhang S (2019) Microglial activation after ischaemic stroke. Stroke Vasc Neurol 4:71–74. https://doi.org/10.1136/svn-2018-000196

Ziemka-Nalecz M, Jaworska J, Zalewska T (2017) Insights into the neuroinflammatory responses after neonatal hypoxia-ischemia. J Neuropathol Exp Neurol 76:644–654. https://doi.org/10.1093/jnen/nlx046

Zwemer CF, Whitesall SE, D'Alecy LG (1995) Hypoxic cardiopulmonary-cerebral resuscitation fails to improve neurological outcome following cardiac arrest in dogs. Resuscitation 29:225–236. https://doi.org/10.1016/0300-9572(94)00848-a